Residential Distribution System Harmonic Compensation Using Priority Driven Droop Controller

Md Shirajum Munir, Yun Wei Li, and Hao Tian

***Abstract*—As renewable energy based distributed generation (DG) units are being increasingly connected throughout today's distribution system, they can be used to mitigate harmonics caused by the wide adoption of nonlinear residential loads. To make the best use of all these DGs' ratings, it is important to develop a method to coordinate DGs' participation efforts in harmonic compensation according to their ratings and locations. Due to the low droop slope for the harmonic controller in DGs, traditional harmonic droop control methods can lead to significant harmonic sharing errors. Also, very limited work has been carried out in literature so far to identify the DGs' compensation priorities according to their locations and power rating. To address this issue, a novel priority-driven, droop-based, selective harmonic compensation scheme is developed in this work. The proposed control scheme improves the harmonic sharing accuracy. The compensation priority design and the way to integrate with droop control is studied. To ensure stability, a virtual impedance model-based stability analysis is also discussed. Analysis, comparisons, and simulation results are used to verify the improvement of compensation performance.**

***Index Terms*—Droop control, harmonic compensation, power sharing accuracy.**

I. Introduction

THE recent upsurge of the use of power electronics based nonlinear residential load is a major challenge for utility companies to maintain harmonic related power quality standards [1]. The collective effect of harmonic current injected to the source by different nonlinear residential loads is substantial [2]–[4] which is leading to extensive waveform distortion in the distribution system. This grid harmonic distortion can lead to dielectric failure of the distribution line cable [5], interference with telephone line [6], shunt power factor correction (PFC) capacitor damage [7], overheat, and loss in electrical machines [8], lifetime reduction of transformer and cables [9], etc.

To solve this harmonic problem, passive power filters (PPFs) and active power filters (APFs) were used traditionally. The operation of PPFs is limited to certain tuned harmonics and grid impedance [10]. Whereas APFs are usually installed at certain locations of the distribution system and not very effective at suppressing harmonic distortion at the residential distribution system due to the dispersed nature of the residential loads. In this situation, the increased adoption of renewable energy source (RES) based distributed generation (DG) systems, e.g., rooftop photovoltaic (PV) and small wind turbine systems can provide an excellent solution to this harmonic problem. These PV and wind turbine systems are connected to the grid through DG-grid interfacing voltage source inverters (VSI). When properly controlled, these DG-grid interfacing inverters can be used to compensate system harmonics as an ancillary service [11–14], utilizing the apparent power rating of the inverters. Due to the intermittent nature of renewable energy [15]–[16] and high cost associated with electrical energy storage [17], proper utilization of available apparent power rating of DG systems is a promising prospect.

Traditionally, conductance-power (*G*-*S*) based droop controllers have been used to control several active power filters in different locations [18]. This system is called distributed active-filter systems (DAFS) where individual APFs compensate harmonics without any communication among themselves. The droop slopes of APFs are designed according to their apparent power ratings, which ensures the even sharing of harmonic compensation workload [19]–[20]. This algorithm is extended to DGs to enable the ancillary harmonic compensation function. But due to the differences between APFs and DGs, the controller design approach of DAFS can cause significant power-sharing errors among DGs due to the assumptions made for APFs are unnecessarily true for DGs. A new droop control design method shall be developed by taking DGs' unique features into account. On top of that, additional power sharing error may be introduced depending on the point-of-connection (POC) voltage distortion (due to feeder impedance) [21]. DGs shall be coordinated to correct the sharing error. This can be realized by small AC signal injection [22] or low bandwidth communications [23]–[24]. However, in these coordinated droop control systems, the same harmonic impedance is generally used for all harmonic orders. And all the DGs participate the compensation based on their power ratings. But depending on the network configuration, prioritizing the compensation of some specific harmonics at certain locations will provide better compensation results [25]–[27]. To optimize the harmonic compensation performance,

Manuscript received July 13, 2020; revised September 2, 2020; accepted September 9, 2020. Date of publication September 30, 2020; date of current version September 24, 2020. This work was supported by Canada First Excellent Research Fund—Future Energy System and Natural Sciences and Engineering Research Council of Canada. *(Corresponding author: Hao Tian.)*

The authors are with the Department of Electrical and Electronic Engineering, University of Alberta, AB T6G 2V4, Canada (email: mdshiraj@ualberta.ca; yunwei.li@ualberta.ca; htian2@ualberta.ca).

Digital Object Identifier 10.24295/CPSSTPEA.2020.00018

it is important to find out the locations in the system that are more prone to voltage distortion, especially when the systems have resonance introduced by the PFC capacitors. Identifying the resonance prone locations and compensating harmonics at those locations with higher priority, it is possible to improve the harmonic compensation performance. In this case, it is necessary to apply different compensation priorities at harmonic orders for DGs at different locations to achieve better harmonic compensation performance throughout the system.

To overcome all these drawbacks associated with traditional *G-S* droop based controller, a novel priority-driven droop controller is proposed in this paper. This method improves the DGs' harmonic compensation from the following two perspectives: i) improving the design method in the primary control; ii) applying priority in the supervisory control. In the primary control layer, the design flaw has been addressed in the proposed controller which eliminates power sharing error. It is revealed that setting droop slope proportional to DGs' apparent power ratings can unnecessarily ensure proper harmonic current sharing. With the modified *G-S* droop controller, a new droop slope design guidance is provided to improve the harmonic sharing accuracy. Also, the power sharing errors introduced by the different amplitudes of POC harmonics are discussed and eliminated in the proposed controller. To improve the overall harmonic compensation performance in the distribution grid, the priorities are applied to DGs at different nodes with the help of supervisory control. In this case, the DGs at the critical nodes can contribute more and the distribution grid will see a more effective harmonic compensation. To identify the harmonic compensation priorities for the proposed droop controller, coordinated control of the DGs operating at different locations is developed where the harmonic compensation priorities are quantified using the sensitivity to resonance data are obtained from the modal analysis [27]. To better implement the modified *G-S* droop control with the priority calculation method, the interface between *G-S* droop controller and the priority identification is designed.

Besides, although the priority-driven *G-S* droop control improves harmonic compensation performance, it is still necessary to check the stability of the proposed control system. To ensure stability, the impedance model of a typical residential distribution system and the DG converters are built. In the detailed impedance models, the detailed controller models are considered. Then the stability of the overall system is checked and the feasibility of the priority-driven droop control system is validated.

The rest of the paper is organized as follows: Section II introduces the traditional droop controller and its limitations. Based on that, the proposed priority-driven conductance-power (*G-S*) based droop control scheme is illustrated. The mitigation technique of power sharing error introduced by the feeder impedance and connection point harmonics are also discussed in this section. Section III discusses the resonance mode and compensation priority calculation technique. To prove the feasibility of this method, a typical residential distribution system model is developed in Section IV, whose stability analysis shows the proposed method can have enough stability margin under proper design. Finally, Section V draws the concluding remarks about this work.

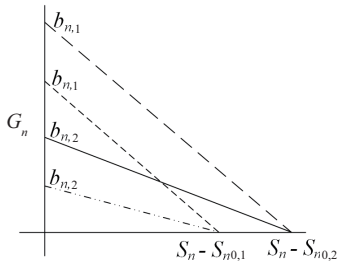

Fig. 1. Conductance vs. power relationship using *G-S* droop control.

II. Modified Conductance-Power (*G-S*) Based Droop Controller

A. Principle of Traditional Conductance-Power Droop

In traditional conductance-power (*G-S*) based droop algorithm [18]–[20], harmonic conductance command is obtained from the output apparent power at harmonic orders (S_n), rated capacity of converters (S_{n0}), droop offset (G_{n0}) and *G-S* droop equation shown in (1) and Fig. 1.

$$G_n = G_{n0} + b_n(S_n - S_{n0}) \tag{1}$$

The harmonic voltage content at POC (V_{G_h}) is modified according to the harmonic conductance command (G_n) to generate the harmonic reference current. Since the main component of the RMS voltage at POC is the fundamental voltage, the output harmonic apparent power of DG (S_n) can be expressed as:

$$S_n = |V_n|G_n|V_{n,h}| \approx |V_{n,f}|G_n|V_{n,h}|. \tag{2}$$

Combining (1) and (2), it is easy to obtain:

$$S_n = |V_{n,f}|[G_{n0} + b_n(S_n - S_{n0})]|V_{n,h}| \tag{3}$$

or

$$S_n = \frac{|V_{n,f}|(G_{n0} - b_n S_{n0})|V_{n,h}|}{1 - b_n|V_{n,f}||V_{n,h}|}. \tag{4}$$

In some previous works [18]–[20], (4) is simplified by assuming $b_n|V_{n,f}||V_{n,h}| >> 1$ as:

$$S_n b_n = b_n S_{n0} - G_{n0}. \tag{5}$$

If there are an n number of DGs and their droop characteristics are assigned as:

$$b_1 S_{10} - G_{10} = b_2 S_{20} - G_{20} = ... = b_n S_{n0} - G_{n0}. \tag{6}$$

Substituting (5) into (6), the following equation can be obtained:

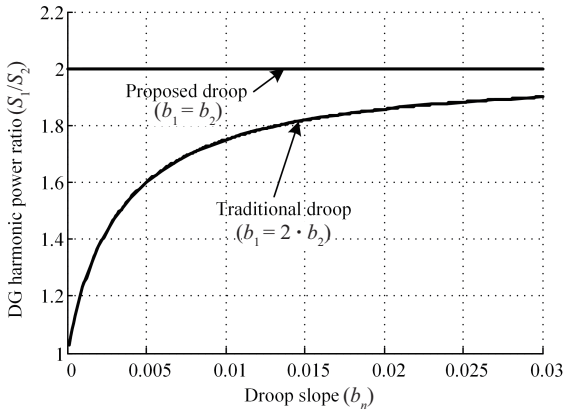

Fig. 2. Power sharing of DGs with traditional and proposed conductance-power droop controller with $G_{n0} = 0$.

$$S_1 b_1 = S_2 b_2 = \ldots = S_n b_n. \tag{7}$$

So, the output harmonic apparent power of the DGs are inversely proportional to the slope of the droop controller according to (7). While the slope of the droop controller is inversely proportional to the apparent power rating of respective DGs according to (6). Combining (6) and (7), it can be seen that such droop slope allocation will allow proportional sharing of the harmonic filtering workload among different DG units according to the respective DG rating as shown in (8).

$$\frac{S_1}{S_{10}} = \frac{S_2}{S_{20}} = \ldots = \frac{S_n}{S_{n0}} \tag{8}$$

Therefore, in traditional DGs, the *G-S* droop controller is designed similarly to the active power-frequency (*P-f*) and reactive power-voltage (*Q-V*) droop. All the slopes are set to be proportional to the apparent power rating.

B. Proposed Conductance-Power Droop for DGs

In the case of the traditional droop controller, (7) is derived assuming $b_n |V_{n,f}||V_{n,h}| >> 1$. As DGs are not dedicatedly designed for harmonic compensation, the available power rating for harmonic compensation is generally lower than APFs, which requires a low droop slope for harmonic sharing. Also, the stability concerns in the residential distribution grid also ask for a low droop slope. As a result, in *G-S* droop controllers for DGs, the droop slope (b_n) can be very small, resulting in that $b_n |V_{n,f}||V_{n,h}| \approx 1$. So, the original assumption — $b_n |V_{n,f}||V_{n,h}| >> 1$ that leads to (6) may not hold valid. Applying the traditional design method will introduce considerable error in harmonic power sharing among different DG units.

To demonstrate this, Fig. 2 shows the output power ratio (S_1/S_2) of 2 DGs with S_{10} = 1000 VA and S_{20} = 500 VA respectively. Here the range of b_2 is double of b_1 since $S_{20} = 2S_{20}$. Now, if b_1 = 0.005 then according to the traditional droop controller, b_2 = 0.01. It can be seen from Fig. 2 that the power sharing accuracy with the traditional droop controller is very poor especially when the droop slope is lower.

To ensure harmonic power sharing accuracy, i.e., ensure the DG harmonic power S_n to be proportional to the DG rating S_{n0}, droop slopes shall be designed with a new method. The new design approach shall consider two situations: i) when conductance offset is zero; ii) when conductance offset is not zero.

1) With Conductance Offset 0 ($G_{n0} = 0$)

If conductance offset is considered 0 ($G_{n0} = 0$) in (4), then (4) can be rewritten as:

$$S_n = \frac{-b_n S_{n0} |V_{n,f}||V_{n,h}|}{1 - b_n |V_{n,f}||V_{n,h}|}. \tag{9}$$

It is easy to find that if fundamental and harmonic voltages are constant at the POC, the harmonic power S_n can be proportional to rated apparent power S_{n0} if the droop slopes of all DGs are the same for all DGs, i.e., if setting b_n = const. for DGs, (9) can be rewritten as:

$$S_n = \text{const} \cdot S_{n0}. \tag{10}$$

To demonstrate this, Fig. 2 shows the output power ratio (S_1/S_2) of 2 DGs with S_{10} = 1000 VA and S_{20} = 500 VA respectively. According to the proposed droop controller, when droop slopes for different DGs are kept the same then the DG outputs should be proportional to the respective DG ratings. It can be seen from Fig. 2 that power sharing is always accurate and independent on the value of b_n.

2) With Nonzero Conductance Offset ($G_{n0} \neq 0$)

According to the traditional droop controller, the conductance offset should be constant across *n* number of DGs to make the droop characteristics relationship shown in (6) valid when ($G_{n0} \neq 0$). But when the droop offset is constant across *n* number of DGs, the output power of all DGs will be the same irrespective of their rating and this will introduce power sharing error. If conductance offset is nonzero ($G_{n0} \neq 0$) while the fundamental and harmonic voltages at POC are constant and droop slopes of all DGs are same for all DGs (b_n = const.) in (4), then (4) can be rewritten as:

$$S_n = \frac{|V_{n,f}|(G_{n0} - b_n S_{n0})|V_{n,h}|}{1 - b_n |V_{n,f}||V_{n,h}|}. \tag{11}$$

To make the DG harmonic power S_n proportional to the DG rating S_{n0}, G_{n0} has to be proportional to DG rating S_{n0} as:

$$G_{n0} = K_G S_{n0}. \tag{12}$$

where K_G is the conductance offset constant and has the same value for all DGs. Then (11) becomes,

$$S_n = S_{n0}(K_G - b_n) \tag{13}$$

or

$$S_n \propto S_{n0}. \tag{14}$$

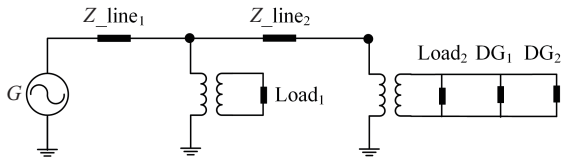

Fig. 3. Test circuit for comparison of power sharing accuracy of the traditional and modified droop controller when DGs are connected to the same node.

TABLE I
CIRCUIT PARAMETERS

Circuit parameters	Value
Grid voltage	7.2 kV
Distribution transformer	7200 V/120 V, (0.015+0.03) j p.u.
Distribution line impedance	0.43 Ω/km, 150 μH/km

TABLE II
COMPARISON OF HARMONIC POWER SHARING ACCURACY AMONG DIFFERENT DGS WITH TRADITIONAL AND PROPOSED CONDUCTANCE-POWER BASED DROOP CONTROLLER

Scenario	S_{10}	S_{20}	S_{20}/S_{10}	b_1	b_2	S_1	S_2	S_2/S_1
(Case 1)	100	400	4.00	0.08	0.02	98.1	380.0	3.87
(Case 2)	100	400	4.00	0.008	0.002	89.2	269.0	3.01
(Case 3)	100	400	4.00	0.0008	0.0002	45.6	69.5	1.51
(Case 4)	100	400	4.00	0.008	0.008	89.2	356.5	4.00
(Case 5)	100	400	4.00	0.0002	0.0002	17.3	69.5	4.00

Again, according to (14), DG output power will be proportional to DG rating when ($K_G + b_n$) is a constant.

C.Verification of the Power Sharing Accuracy of the Proposed Droop Controller

To show how the proposed droop controller will ensure proper power sharing, two DGs are considered to be operating at the same POC, where $S_{10} = nS_{20}$. So, DG power outputs should be $S_1 = nS_2$ and the conductance relationship should be $G_1 = nG_2$. Then simulation uses the circuit configuration shown in Fig. 3 and parameters listed in Table I. Here a single residential house load model is used as each load. The results are listed in Table II. As shown in Table II, the power sharing is accurate with (14) unlike with (4). As the droop slope is lowered, the sharing error becomes greater. On the other hand, power sharing remains very accurate with the modified droop controller even with a very low droop slope (case 5).

D.Mitigation of Power Sharing Error Introduced by Feeder Impedance

It should be noted here that the proposed droop controller is implemented using (14) where the apparent power at different nodes (S_n) is calculated using (4). Now, the fundamental component of the line voltage is almost the same at different

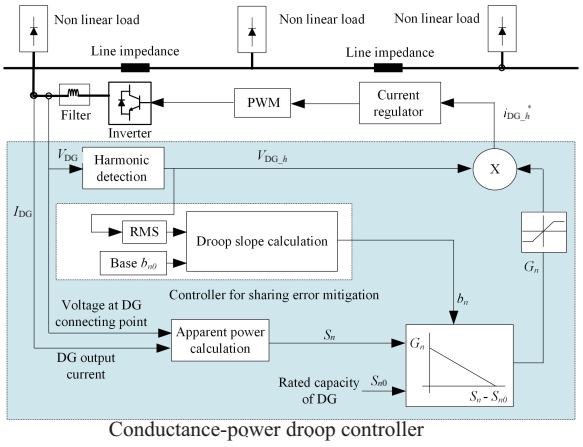

Fig. 4. Block diagram of the modified droop controller with constant $b_n \cdot V_{n,h}$ controller.

POC throughout the distribution system. But the node harmonic voltage at different nodes ($V_{n,h}$) can vary due to the feeder impedance of the distribution system. As a result, sharing error may be introduced even when the proposed droop controller is used. This sharing error increases with the increase of the droop slope. This can be explained using (4). It can be seen from (4) that a higher droop slope will try to increase DG harmonic power S_n. Increasing harmonic power S_n will result in lower harmonic voltage ($V_{n,h}$) at the POC, and the variations in harmonic voltage can be different at different nodes. Moreover, the DG systems are usually connected to the secondary side of the distribution transformer. Since the transformer impedance is much higher compared to distribution line impedance, the voltage distortion difference can be significant at POC of different DGs, further increasing the sharing error.

The sharing error can be removed by implementing an additional control block that automatically adjusts the droop slope in a small range according to the node harmonic voltage ($V_{n,h}$) variation using (15).

$$\bigcup_{h=3,5,\ldots}^{h_{\max}} b_{n,h} = \frac{b_{n0,h} V_{n0,h,\mathrm{rms}}}{V_{n,h,\mathrm{rms}}} \tag{15}$$

Here, $b_{n0,h}$ is the base droop slope at different harmonics $V_{n0,h,\mathrm{rms}}$, and $V_{n,h,\mathrm{rms}}$ is the h^{th} harmonic voltage at the n^{th} node. By doing this, $b_{n,h} \cdot V_{n,h}$ of (4) will become a constant and remove any effect of varying $V_{n,h}$ on sharing error Fig. 4 shows the implementation of the proposed droop controller which mitigates the effect of POC harmonics. As can be seen, the rms value of voltage harmonics is extracted and the droop slope for each order harmonics is modified according to (15). This modifies the droop slope b_n designed with the guidance provided in Section II B in a small range. With the proposed *G-S* droop, the harmonic current reference can be generated and executed by the inner current regulator. It is worth noting that this implementation is equivalent to virtual impedance control. The conductance *G* is the reciprocal of virtual impedance. The performance can be seen from Fig. 5, in traditional droop

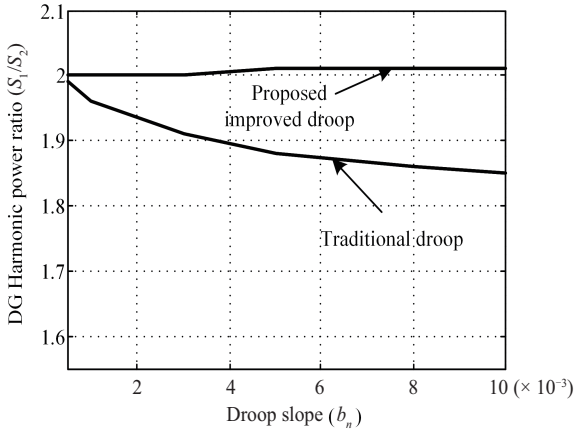

Fig. 5. Power sharing error introduced by feeder impedance and mitigation of that error using the proposed improved droop controller.

control, the sharing error increases when the droop slope increases. On the other hand, due to the measures to mitigate the impact of line impedance and varying harmonic voltage, the proposed droop controller ensures the harmonic power can be properly shared.

III. Implementation of the Modified Conductance-Power Based Priority Driven Droop Controller

As discussed in Section II, the proposed droop controller can eliminate power sharing error among different DGs operating at different nodes in the distribution system. The harmonic compensation performance can still be further improved. Harmonic compensation priorities at different nodes and at different harmonic frequencies can be applied. This can control the DGs at the critical nodes to contribute more on harmonic compensation at specific harmonic order.

To apply priorities to the proposed droop, the priorities shall be identified first. Then the proposed droop controller can be realized using those identified priority values. However, the droop equation shown in (1) has variables, which can be modified to implement the priority. These variables are, droop slope (b_n), conductance offset (G_{n0}), and DG rated capacity (S_{n0}). It is necessary to find the best way to implement the priority in the proposed *G-S* droop control. In this section, the harmonic compensation priorities will be identified first and then the droop variables will be analyzed to see which one is most suitable. Then the proposed droop controller will be implemented using the selected modified variable for better compensation results.

A. Resonance Mode Analysis and Priority Calculation

To carry out frequency scan analysis, an electrical network of n node is represented by an $n \times n$ admittance matrix $[Y]$ at first. Then the voltage vector of the system is calculated from

$$[V]_f = [Z_N]_f [I]_f \tag{16}$$

Here, $[V]$, $[Z_N]$ and $[I]$ are nodal voltage vector, nodal impedance and nodal current vector respectively while subscript f denotes the frequency. The modal analysis will be used here to identify the component and bus that excites the resonance using (17)

$$\underbrace{\begin{bmatrix} V_{m,1} \\ V_{m,2} \\ \vdots \\ V_{m,N} \end{bmatrix}_f}_{\text{Modal voltage}} = \underbrace{\begin{bmatrix} Z_{m,11}^{-1} & 0 & \vdots & 0 \\ 0 & Z_{m,22}^{-1} & \vdots & 0 \\ \vdots & \vdots & \vdots & 0 \\ 0 & 0 & 0 & Z_{m,NN}^{-1} \end{bmatrix}_f}_{\text{Modal impedance}} \underbrace{\begin{bmatrix} i_{m,1} \\ i_{m,2} \\ \vdots \\ i_{m,N} \end{bmatrix}_f}_{\text{Modal current}} \tag{17}$$

Here,

$$[Z_M]_f = [L]_f^{-1} [Z_N]_f [T]_f^{-1} \tag{18}$$

Wherein, $[Z_M]$ is the diagonal eigenvalue matrix. $[L]$ is the left eigenvalue matrix and while $[T]$ is the right eigenvalue matrix. With the transformation defined in (18), the nodal impedance $[Z_N]$ is transformed into modal impedance $[Z_M]$ in (17), which is a diagonal matrix.

In the modal impedance matrix $[Z_M]$, the critical modal impedance is much higher than other modal impedances. The low impedance can be ignored and the diagonal matrix can be simplified to be a sparse matrix, as shown in (19).

$$\underbrace{\begin{bmatrix} Z_{m,11}^{-1} & 0 & \vdots & 0 \\ 0 & Z_{m,22}^{-1} & \vdots & 0 \\ \vdots & \vdots & \vdots & 0 \\ 0 & 0 & 0 & Z_{m,NN}^{-1} \end{bmatrix}_f}_{\text{Modal impedance}} \approx \underbrace{\begin{bmatrix} Z_{m,11}^{-1} & 0 & \vdots & 0 \\ 0 & 0 & \vdots & 0 \\ \vdots & \vdots & \vdots & 0 \\ 0 & 0 & 0 & 0 \end{bmatrix}_f}_{\text{Modal impedance}} \tag{19}$$

Combining (17)–(19), (20) can be obtained:

$$\begin{bmatrix} V_1 \\ V_2 \\ \vdots \\ V_N \end{bmatrix}_f = Z_{m,11,f}^{-1} \underbrace{\begin{bmatrix} L_{11}T_{11} & L_{12}T_{12} & \vdots & \vdots \\ L_{21}T_{11} & L_{22}T_{12} & \vdots & \vdots \\ \vdots & \vdots & \vdots & \vdots \\ \vdots & \vdots & \vdots & L_{N1}T_{1N} \end{bmatrix}_f}_{\text{Particapation factor}} \begin{bmatrix} I_1 \\ I_2 \\ \vdots \\ I_N \end{bmatrix}_f . \tag{20}$$

The participation factor (PF) matrix of (20) denotes the impact of each bus on the critical mode. Whereas $Z_{m,11,f}^{-1}$ denotes the impact level at different harmonic frequencies. Combining the modal impedance and PF index, one can determine the participation effort of each bus to output harmonic voltage distortion. In this work, this approach will be used to quantify the harmonic compensation priorities at different harmonic frequencies and at different nodes of the distribution system.

B. Analysis of the Variables of the Droop Controller

As mentioned before, the droop equation has three variables that can be modified to implement the compensation priority and obtain improved harmonic compensation performance. In

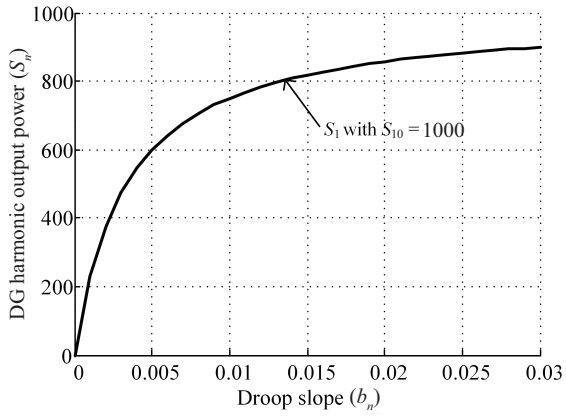

Fig. 6. Variation of DG output power (S_1) with different droop slopes (b_n), zero conductance offset (G_{n0} = 0), and same DG rating (S_{10} = const.).

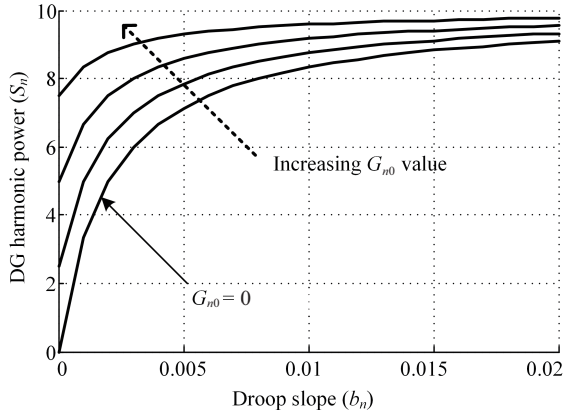

Fig. 7. DG output power variation with varying droop slope offset (G_{n0}) and the same DG rating (S_{10} = const.).

this section, these variables are analyzed to identify the most suitable one for implementing the proposed priority-driven droop controller.

1) Modification of Droop Slope (b_n)

Fig. 6 shows the variation of DG output harmonic power with different droop slope (b_n) under the same DG rating (S_{n0}) and zero conductance offset (G_{n0} = 0). To apply the priority by changing the droop slope, it is necessary to change the droop slope in a linear range (0 to 0.03 in this case) according to the expected priorities from the modal analysis. However, as can be seen from Fig. 6, when the droop slope is low (e.g., lower than 0.005), the ratio of DG output harmonic power is very low and most of the DG rating will remain unused. On the other hand, when the droop slope value is high (e.g., larger than 0.015), the output DG power remains almost constant even if the droop slope is changed. This significant nonlinearity makes it difficult to tune the priority. So, modifying the droop slope according to the compensation priority value is not ideal.

2) Modification of Conductance Offset (G_{n0})

Fig. 7 shows the relationship between DG output harmonic power and droop slope under different conductance offset (b_n)

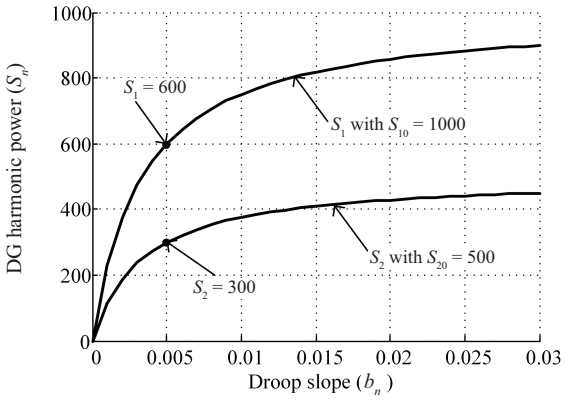

Fig. 8. DG output power variation with varying DG rating (S_{n0}).

while setting the same DG rating (S_{n0}) It can be seen from this figure that changing the conductance offset (G_{n0}) can change the priority. DGs will generate different harmonic power under the different conductance offset. However, when the conductance offset is used, the harmonic power is not zero even when the droop slope is zero. So, using nonzero values for conductance offset can cause DG overloading—the harmonic power can add up to the fundamental power and exceeds the designed total power rating. Hence, modifying conductance offset (G_{n0}) according to identified compensation priority values is not ideal either.

Fig. 8 shows the variation of DG harmonic power with zero conductance offset (G_{n0} = 0), same droop slope (b_n), and different DG ratings (S_{n0}). As can be seen, DG output can be effectively controlled using different DG rating values in the droop equation. For example, when S_{20} is reduced by 50% of S_{10}, the DG output S_2 is also reduced by 50% of S_{10} when the same droop slope is used. The power sharing is accurate in this case and this holds valid for entire range of droop slope. Hence, it is recommended to modify DG rating for harmonic at different nodes and at different harmonic orders according to the identified priority values. As DG is not dedicatedly for harmonic compensation, the harmonic rating is changing under different conditions. Changing the available rating to realize priority will not impact the function of the DG.

C. Implementation and Verification

Finally, the modified droop controller is implemented with droop parameters obtained using modal analysis. To validate the method, the modal analysis is carried out on an 11-node system with a PFC capacitor at node 7. The obtained compensation priority values (CPV) are listed in Table III.

According to the discussion in Section III B, the priority shall be implemented by changing the available power rating for harmonic compensation at each harmonic order and at each node. If the available DG ratings of different DGs are S_{n0} then the reference DG ratings (S_{n0}^*) can be identified. Here, the DG with the highest priority will use most of its rating for harmonic small portion of its rating for harmonic compensation. DGs will effectively utilize their power ratings and will not be

TABLE III
DG COMPENSATION PRIORITY VALUES (PV)

Priorities at node	Harmonic order						
	3rd	5th	7th	9th	11th	13th	15th
1	0.08	0.17	0.37	0.38	0.19	0.11	0.07
2	0.10	0.21	0.46	0.47	0.24	0.14	0.09
3	0.12	0.25	0.55	0.57	0.30	0.18	0.12
4	0.14	0.29	0.64	0.67	0.35	0.22	0.15
5	0.15	0.32	0.72	0.78	0.42	0.26	0.19
6	0.17	0.36	0.81	0.89	0.49	0.32	0.23
7	0.18	0.39	0.89	1.00	0.57	0.38	0.29
8	0.19	0.40	0.90	0.98	0.54	0.35	0.25
9	0.19	0.41	0.91	0.97	0.51	0.32	0.22
10	0.20	0.41	0.91	0.96	0.50	0.30	0.20
11	0.20	0.42	0.91	0.95	0.49	0.29	0.19

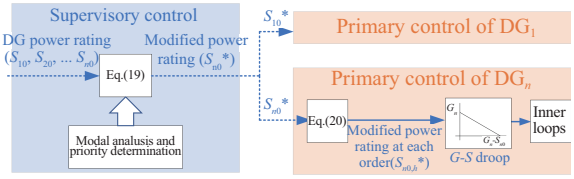

Fig. 9. Block diagram of the priority-driven droop controller.

overloaded. In practice, the priority will be determined in the supervisory controller. Once the reference harmonic power ratings (S_{n0}^*) is identified, the modified power rating for different harmonic orders will be distributed to the DGs at different nodes. This is shown in Fig. 9 and (21)–(22).

$$S_{n0}^* = S_{n0} \frac{\sum_{h=3,5,7...}^{h_{max}} PV_{k,h}}{\sum_{n=1,2,3...}^{N} \sum_{h=3,5,7...}^{h_{max}} PV_{n,h}} \tag{21}$$

Where, $PV_{k,h}$ is the priority for node k and harmonic order h.

For individual harmonic order, the available power rating can be calculated by (22):

$$S_{n0,h}^* = S_{n0}^* \frac{PV_{k,h}}{\sum_{h=3,5,7...}^{h_{max}} PV_{k,h}} \tag{22}$$

The priority value $PV_{k,h}$ can be calculated as:

$$PV_{k,h} = \frac{PF_{k,h} Z_{k,h} H_{k,h}}{\max\left[\bigcup_{n,h}^{n=1,2,..N;\, h=3,5,..h_{max}} (PF_{n,h} Z_{n,h} H_{n,h})\right]} \tag{23}$$

The priority values at different nodes and different harmonics $PV_{k,h}$ are obtained from the priority from critical modal impedance ($Z_{n,h}$), priority from load harmonic data ($H_{n,h}$), and priority from participation factor ($PF_{n,h}$) in (20).

The compensation results with different methods are shown in Fig. 10. For a fair comparison, harmonic compensation is

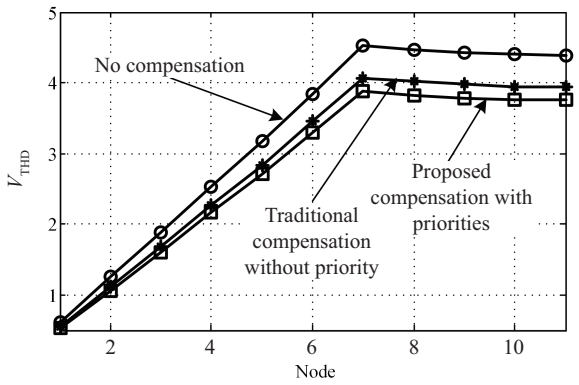

Fig. 10. V_{THD} values at different distribution system nodes using different compensation schemes.

carried out using traditional and proposed droop controller while keeping the total capacity the same. As shown in Fig. 10, the voltage harmonic amplitude at each node is lower when the proposed droop controller is used.

It is worth noting that modal analysis requires information about impedances and structure of the distribution grid. Considering the development of the smart grid and Internet-of-things, this information is getting easier to obtain in the modern distribution grid. Therefore, the proposed priority-based compensation targeting on improving overall total harmonic distortion (THD) shows great potential in the foreseeable future.

IV. IMPEDANCE MODEL AND STABILITY ANALYSIS

With the modified droop controller integrated priority, the harmonic compensation in a residential system can be improved. However, stability can still be a challenge. In this section, the dynamic behavior of an N node distribution system will be investigated to determine the stability range. The analysis is based on the impedance model. To do so, a typical distribution system with DG is modeled first, and then, stability analysis was carried out using the developed model.

A. Impedance Model of DG

To facilitate the stability analysis, the DGs will be modeled as impedance according to is conductance/impedance at each harmonic order. This is based on the fact that the modified *G-S* droop uses harmonic voltage to determine the current references, i.e., $I_h^* = V_{G\_h}^* G_h$. This is equivalent to $I_h^* = V_{G\_h}/R_h$. Therefore, under the proposed *G-S* droop control, the reference harmonic current for multiple harmonic orders can be obtained by combining all the individual harmonic references as:

$$I_h^* = I_3^* + I_5^* + ... + I_{15}^*. \tag{24}$$

The block diagram of the DG unit is shown in Fig. 11. In this work, every individual harmonic component of DG output current will be controlled to get improved harmonic compensation results. The equivalent virtual resistance at each

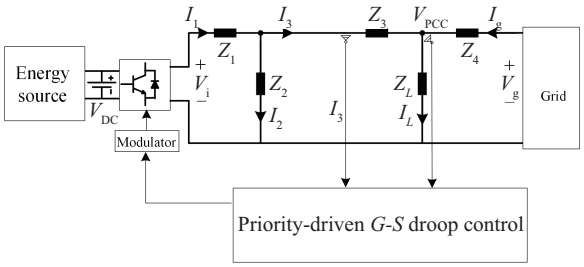

Fig. 11. System model for the DG converter controlled by the priority-driven *G-S* droop.

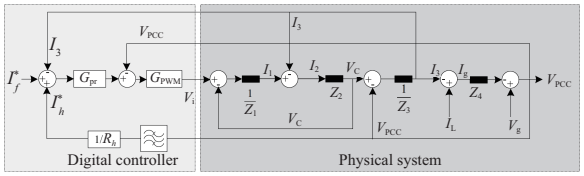

Fig. 12. Equivalent block diagram of the inverter controller with virtual harmonic resistance and conductance-power droop controller.

harmonic order can be obtained according to the conductance used in the harmonic control system. For fundamental current tracking and harmonic current control, P+ resonant controllers are used [28]–[29]. To improve the dynamic response and stability of the control loop, a proportional controller is usually adopted for the inner filter inductor current feedback loop.

The average model is employed in this paper. The DG output is assumed to be proportion to the modulation index. The non-linearity is neglected while the accuracy is acceptable as the frequency of low order harmonics is much lower than the switching frequency of DGs [30]–[31].

Fig. 12 shows the equivalent block diagram of the inverter controller. This inverter controller can be expressed as the Norton equivalent circuit in (25).

$$I_3 = V_{\mathrm{PCC}} Y_{\mathrm{eq},h} + I_f^* G_{\mathrm{eq}} \tag{25}$$

where,

$$Y_{\mathrm{eq},h} = \frac{(1 + sC_f R_d)(G_{\Sigma h} G_{\mathrm{PWM}} G_{\mathrm{PR},h} + G_{\mathrm{PWM}} - 1) - L_1 C_f s^2}{(G_{\mathrm{PWM}} G_{\mathrm{PR},h} + L_1 s - L_2 s)(1 + sC_f R_d) - L_1 L_2 C_f s^3} \tag{26}$$

and,

$$G_{\mathrm{eq}} = \frac{G_{\mathrm{PWM}} G_{\mathrm{PR},h} (1 + sC_f R_d)}{(G_{\mathrm{PWM}} G_{\mathrm{PR},h} + L_1 s - L_2 s)(1 + sC_f R_d) - L_1 L_2 C_f s^3}. \tag{27}$$

The PWM delay [32] can be included without introducing non-linearity by using 2nd order Padé approximation. In this case, the G_{PWM} shall be $V_{\mathrm{dc}}/2 \cdot G_{\mathrm{delay}}$. And G_{delay} is defined as:

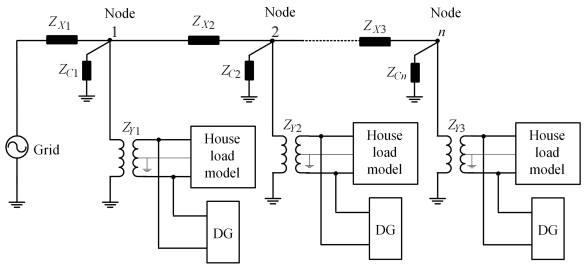

Fig. 13. Simplified single distribution feeder.

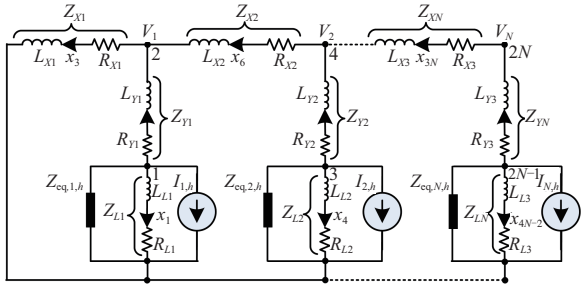

Fig. 14. Equivalent model of an *N* node distribution feeder with virtual harmonic impedance.

$$G_{\mathrm{delay}}(s) = \frac{1 - \frac{t}{2}s + \frac{t^2}{12}s^2}{1 + \frac{t}{2}s + \frac{t^2}{12}s^2}, \tag{28}$$

where t is half of the switching period [13].

B. Distribution System Modeling

To model a distribution system, residential house loads are modeled using the harmonic load data [33]–[34]. The distribution system used in this work has a 34.4 kV transmission line which is connected to the 12.47 kV distribution feeders through a transmission transformer (Xf_{tr}) [35]. The 3 phase distribution feeder has 11 nodes. On each node, a group of 12 houses is connected to the distribution feeder through a distribution transformer (Xf_{dis}) in a way that the load current is balanced [36]–[37]. To investigate the effectiveness of different harmonic compensation schemes, a distribution bus with PFC capacitors is considered [38]–[39].

In Fig. 13, DGs are connected at the secondary side of the distribution transformer. In this model, n = 1, 2, 3…, N represents the n^{th} node. Z_{Xn} represents the distribution line impedance, Z_{Yn} represents the distribution transformer impedance.

The equivalent model of the system in Fig. 13 is shown in Fig. 14. Here, V_n is the voltage at the n^{th} node. x_1, x_4, …, x_{3N-2} are the currents through Z_{L1}, Z_{L2}, …, Z_{Ln}. x_2, x_5, …, x_{3N-1} are the currents through Z_{Yn}. x_3, x_6, …, x_{3N} are the currents through Z_{Xn}. Here, x_1, x_2, …, x_{3N} are taken to be the state variables, I_{hn} is the input, and V_n is the output of the state-space model of the system. Then for an N-node system, there are $3N$ state equations. The $1-N$, $N+1$ to $2N$, and $2N+1$ to $3N$

equations are shown in (29)–(31), respectively:

$$\bigcup_{n=1}^{N} n \rightarrow I_{h\cdot n} = x_{3n-2} + x_{3n-1} + \frac{x_{3n-2}R_{L\cdot n} + \dot{x}_{3n-2}L_{L\cdot n}}{R_n} \quad (29)$$

$$\bigcup_{n=1}^{N} N+n \rightarrow \sum_{n=1}^{N}\left(x_{3\cdot n}R_{X\cdot n} + \dot{x}_{3\cdot n}L_{X\cdot n}\right) - x_{3n-1}R_{Y\cdot n} - \dot{x}_{3n-1}L_{Y\cdot n} = x_{3n-2}R_{L\cdot n} + \dot{x}_{3n-2}L_{L\cdot n} \quad (30)$$

$$\bigcup_{n=1}^{N} 2N+n \rightarrow x_{3n-1} + x_{3n+3} = x_{3n} \quad (31)$$

Solving (29) to (31) yields the A_N and B_N matrices of the state space model while the equation of the system output yields the C_N and D_N matrices of the state-space model.

$$\bigcup_{n=1}^{N} v_n = v_{n-1} + x_{3n}R_{Xn} + \dot{x}_{3n}L_{Xn} \quad (32)$$

Hence, the state-space model of the system can be obtained as shown in (33).

$$\frac{v_n(s)}{I_{hn}(s)} = C_N \phi B_N + D_N \quad (33)$$

where, $\varphi = (sI - A_N)^{-1}$, $n = 1, 2, \ldots, N$, and I is a $3N \times 3N$ identity matrix. For a typical dynamic behavior analysis, a 2 node system is considered in this work. To simplify the analysis, $Z_{x1} = Z_{x2} = Z_x$, $Z_{Y1} = Z_{Y2} = Z_Y$, $Z_{L1} = Z_{L2} = Z_L$ and $I_{h1} = I_{h2} = I_h$ is assumed. Then,

$$\frac{V_1}{I_h} = \frac{Z_X Z_Y Z_2 + 2Z_X Z_1 Z_2 + Z_X^2 Z_1 + Z_X Z_Y Z_1}{\left[\begin{array}{l} Z_Y^2 + 3Z_X Z_Y + Z_X^2 + \left(2Z_X + Z_Y\right)Z_1 \\ +\left(Z_X + Z_Y\right)Z_2 + Z_1 Z_2 \end{array}\right]} \quad (34)$$

and,

$$\frac{V_2}{I_h} = \frac{Z_X Z_Y Z_1 + \left(Z_X^2 + 2Z_X Z_1\right)Z_2 + 3Z_X Z_1 Z_2}{\left[\begin{array}{l} Z_Y^2 + 3Z_X Z_Y + Z_X^2 + \left(2Z_X + Z_Y\right)Z_1 \\ +\left(Z_X + Z_Y\right)Z_2 + Z_1 Z_2 \end{array}\right]} \quad (35)$$

where,

$$Z_{\text{eq1(2)}} = \frac{\left(R_L + sL_L\right)Z_{\text{eq1(2),}h}(s)}{R_L + sL_L + Z_{\text{eq1(2),}h}(s)} \quad (36)$$

C. Stability Analysis

Using (34) and (35), stability analysis can be carried out. Fig. 15 shows the root locus analysis for 3rd harmonic with DG at node 1. It can be seen from Fig. 15 that the system is stable when $R_{1,3} > 0.0043\ \Omega$. Similarly, the minimum R_V for each dominant harmonic frequency and each compensation strategy

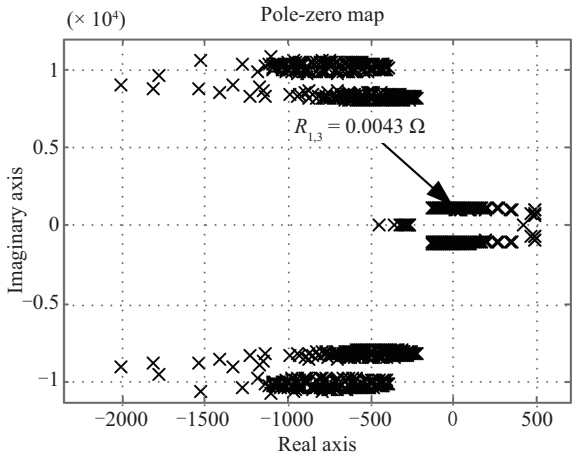

Fig. 15. Root locus analysis for 3rd harmonic with DG at node 1.

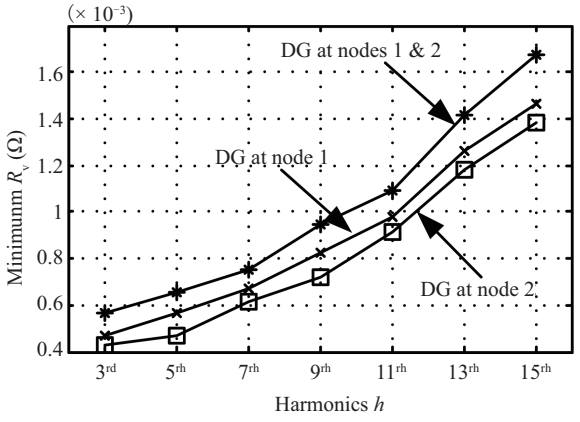

Fig. 16. Minimum R_V for each dominant harmonics when different compensation strategies are used.

can be obtained (DG at node 1, DG at node 2, and finally DG at both node 1 and node 2) from stability analysis and are shown in Fig. 16.

It can be seen from Fig. 16 that different positions of DG in the distribution system can impact the stability of the system. When the DG is installed at node 2, the minimum virtual harmonic resistance is lower than the case when DG is connected at node 1. And when DG is connected at both nodes 1 and 2, the required minimum virtual harmonic resistance is the highest among all these compensation methods. So, it can be concluded that the stability margin is the largest when the end of line compensation is used and the smallest stable region is obtained when distributed compensation is used. It can be seen from Fig. 16 that the minimum R_V changes between 0.0004 Ω to 0.0016 Ω for the different harmonic orders. This corresponds to a max droop slope (b_n) of $-2.5\ \text{V}^{-2}$ to $-0.625\ \text{V}^{-2}$ when the rating is 1000 VA. In the simulation, the base droop slope is $-5 \times 10^{-3}\ \text{V}^{-2}$ which is well within the maximum droop slope range obtained from stability analysis to avoid instability problem. Therefore, it is feasible to use the priority-driven *G-S* droop to improve harmonic compensation performance as a

rational stability range can be found for the proposed control scheme.

V. Conclusion

In this paper, a conductance-power droop based selective harmonic compensation scheme using DG-grid interfacing inverters is developed that improves the harmonic compensation performance on a residential distribution system. The conductance-power droop modifies the droop slope design method and improves the harmonic sharing accuracy. Based on the improved droop controller, harmonic compensation priorities for different DG position and harmonic frequency are identified for improved compensation performance. To implement the compensation priorities, harmonic power ratings of the DG-grid interfacing inverters are modified according to the priority. As a result, selective harmonic compensation can be properly shared according to the power rating, locations, system structure. Also, the stability of the system can be ensured if the control parameters are properly designed. An in-depth analysis, comparison, and simulation of the developed compensation scheme with different existing harmonic compensation schemes were conducted to identify the performance improvement.

References

[1] IEEE Recommended Practices & Requirements for Harmonic Control in Electrical Power Systems, IEEE Standard 519-2014.

[2] R. Dwyer, A. K. Khan, M. Mcgranaghan, L. Tang, R. K. Mccluskey, R. Sung, T. Houy, "Evaluation of harmonic impacts from compact fluorescent lights on distribution systems," in *IEEE Transactions on Power Systems*, vol. 10, no. 4, pp. 1772–1779, Nov. 1995.

[3] F. Nejabatkhah, Y. W. Li, and H. Tian, "Power quality control of smart hybrid AC/DC microgrids: An overview," in *IEEE Access*, vol. 7, pp. 52295–52318, 2019.

[4] N. R. Watson, T. L. Scott, and S. J. J. Hirsch, "Implications for distribution networks of high penetration of compact fluorescent lamps," in *IEEE Transactions on Power Delivery*, vol. 24, no. 3, pp. 1521–1528, Jul. 2009.

[5] D. Salles, C. Jiang, W. Xu, W. Freitas, and H. Mazin,"Assessing the collective harmonic impact of modern residential loads–Part I: method," in *IEEE Transactions on Power Delivery*, vol.27, no.4, pp.1937–1946, Oct. 2012.

[6] J. Arrillaga and N. R. Watson, Power System Harmonics, 2nd ed. Hoboken, NJ, USA: Wiley, 2003, pp. 176–180.

[7] M. H. Shwedhi and M. R. Sultan, "Power factor correction capacitors; essentials and cautions," in *Proceedings of 2000 Power Engineering Society Summer Meeting (Cat. No.00CH37134)*, Seattle, WA, 2000, pp. 1317–1322, vol. 3.

[8] J. H. Seo, T. K. Chung, C. G. Lee, S. Y. Jung, and H. K. Jung, "Harmonic iron loss analysis of electrical machines for high-speed operation considering driving condition," in *IEEE Transactions on Magnetics*, vol. 45, no. 10, pp. 4656–4659, Oct. 2009.

[9] D. C. L. Silva, R. H. Sousa, F. K. A. Lima, and C. G. C. Branco, "Contributions to the study of energy efficiency in dry-type transformer under nonlinear load," in *Proceedings of 2015 IEEE 24th International Symposium on Industrial Electronics (ISIE)*, Buzios, 2015, pp. 456–461.

[10] M. T. Au and J. V. Milanovic, "Planning approaches for the strategic placement of passive harmonic filters in radial distribution networks," in *IEEE Transactions on Power Delivery*, vol.22, no.1, pp.347–353, Jan. 2007.

[11] J. He, B. Liang, Y. W. Li, and C. Wang, "Simultaneous microgrid voltage and current harmonics compensation using coordinated control of dual-interfacing converters," in *IEEE Transactions on Power Electronics*, vol. 32, no. 4, pp. 2647–2660, Apr. 2017.

[12] J. He, Y. W. Li, and M. S. Munir, "A flexible harmonic control approach through voltage-controlled DG–grid interfacing converters," in *IEEE Transactions on Industrial Electronics*, vol. 59, no. 1, pp. 444–455, Jan. 2012.

[13] H. Tian, Y. W. Li, and P. Wang, "Hybrid AC/DC system harmonics control through grid interfacing converters with low switching frequency," in *IEEE Transactions on Industrial Electronics*, vol. 65, no. 3, pp. 2256–2267, Mar. 2018.

[14] S. Munir and Y. W. Li, "Residential distribution system harmonic compensation using PV interfacing inverter," in *IEEE Transactions on Smart Grid*, vol. 4, no. 2, pp. 816–827, Jun. 2013.

[15] A. Capasso, W. Grattieri, R. Lamedica, and A. Prudenzi, "A bottom-up approach to residential load modeling," in *IEEE Transactions on Power Systems*, vol. 9, no. 2, pp. 957–964, May 1994.

[16] C. H. Lin, W. L. Hsieh, C. S. Chen, C. T. Hsu, and T. T. Ku, "Optimization of photovoltaic penetration in distribution systems considering annual duration curve of solar irradiation," in *IEEE Transactions on Power Systems*, vol. 27, no. 2, pp. 1090–1097, May 2012.

[17] M. Subkhan and M. Komori, "New concept for flywheel energy storage system using SMB and PMB," in *IEEE Transactions on Applied Superconductivity*, vol. 21, no. 3, pp. 1485–1488, Jun. 2011.

[18] P. T. Cheng and T. L. Lee, "Distributed active filter systems (DAFSs): A new approach to power system harmonics," in *IEEE Transactions on Industry Applications*, vol. 42, no. 5, pp. 1301–1309, Sep.-Oct. 2006.

[19] T. L. Lee, P. T. Cheng, H. Akagi, and H. Fujita, "A dynamic tuning method for distributed active filter systems," in *IEEE Transactions on Industry Applications*, vol. 44, no. 2, pp. 612–623, Mar.-Apr. 2008.

[20] T. L. Lee and P. T. Cheng, "Design of a new cooperative harmonic filtering strategy for distributed generation interface converters", in *IEEE Transactions on Power Electronics*, vol. 22, no. 5, pp. 1919–1927, Sep. 2007.

[21] J. He, Y. Pan, B. Liang, and C. Wang, "A simple decentralized islanding microgrid power sharing method without using droop control," in *IEEE Transactions on Smart Grid*, vol. 9, no. 6, pp. 6128–6139, Nov. 2018.

[22] B. Liu, Z. Liu, J. Liu, R. An, H. Zheng, and Y. Shi, "An adaptive virtual impedance control scheme based on small-AC-signal injection for unbalanced and harmonic power sharing in islanded microgrids," in *IEEE Transactions on Power Electronics*, vol. 34, no. 12, pp. 12333–12355, Dec. 2019.

[23] T. V. Hoang and H. Lee, "Accurate power sharing with harmonic power for islanded multibus microgrids," in *IEEE Journal of Emerging and Selected Topics in Power Electronics*, vol. 7, no. 2, pp. 1286–1299, Jun. 2019.

[24] H. R. Baghaee, M. Mirsalim, G. B. Gharehpetian, and H. A. Talebi, "Unbalanced harmonic power sharing and voltage compensation of microgrids using radial basis function neural network-based harmonic power-flow calculations for distributed and decentralised control structures," in *IET Generation, Transmission & Distribution*, vol. 12, no. 7, pp. 1518–1530, 10 4 2018.

[25] M. Bradt, B. Badrzadeh, E. Camm, D. Mueller, J. Schoene, T. Siebert, T. Smith, M. Starke, and R. Walling, "Harmonics and resonance issues in wind power plants," in *Proceedings of 2011 IEEE Power and Energy Society General Meeting*, Detroit, MI, USA, 2011, pp. 1–8.

[26] W. Xu, Z. Huang, Y. Cui, and H. Wang, "Harmonic resonance mode analysis," in *IEEE Transactions on Power Delivery*, vol.20, no.2, pp.1182–1190, Apr. 2005.

[27] M. S. Munir, Y. W. Li, and H. Tian, "Improved residential distribution system harmonic compensation scheme using power electronics interfaced DGs," in *IEEE Transactions on Smart Grid*, vol. 7, no. 3, pp. 1191–1203, May 2016.

[28] Y. W. Li and C. N. Kao, "An accurate power control strategy for power-electronics-interfaced distributed generation units operating in a low-voltage multibus microgrid," in *IEEE Transactions on Power Electronics*, vol. 24, pp. 2977–2988, Dec. 2009.

[29] J. He and Y. W. Li, "Analysis, design and implementation of virtual impedance for power electronics interfaced distributed generation," in *IEEE Transactions on Industry Applications*, vol. 47, pp. 2525–2538, Dec. 2011.

[30] H. Tian, Y. W. Li, and Q. Zhao, "Multirate harmonic compensation control for low switching frequency converters: Scheme, modeling, and

analysis," in *IEEE Transactions on Power Electronics*, vol. 35, no. 4, pp. 4143–4156, Apr. 2020.

[31] X. Wang, F. Blaabjerg, and W. Wu, "Modeling and analysis of harmonic stability in an AC power-electronics-based power system," in *IEEE Transactions on Power Electronics*, vol. 29, no. 12, pp. 6421–6432, Dec. 2014

[32] H. R. Baghaee, M. Mirsalim, G. B. Gharehpetian, and H. A. Talebi,"A generalized descriptor-system robust H ∞ control of autonomous microgrids to improve small and large signal stability considering communication delays and load nonlinearities," in *International Journal of Electrical Power & Energy Systems*, vol. 92, pp. 63–82, 2017.

[33] A. B. Nassif, J. Yong, and W. Xu, "Measurement-based approach for constructing harmonic models of electronic home appliances," in *IET Generation, Transmission & Distribution*, vol. 4, no. 3, pp. 363–375, Mar. 2010.

[34] R. Dwyer, A. K. Khan, M. Mcgranaghan, L. Tang, R. K. Mccluskey, R. Sung, and T. Houy, "Evaluation of harmonic impacts from compact fluorescent lights on distribution systems," in *IEEE Transactions on Power Systems*, vol. 10, no. 4, pp. 1772–1779, Nov. 1995.

[35] Y. Wang, R. M. O' Connell, and G. Brownfield, "Modeling and prediction of distribution system voltage distortion caused by residential loads," in *IEEE Transactions on Power Delivery*, vol.16, no.4, pp.744–751, Oct. 2001.

[36] IEEE Guide for the Application of Neutral Grounding in Electrical Utility Systems, Part IV-Distribution, IEEE Standard C62.92.4-1991, 1992.

[37] IEEE Application Guide for IEEE Standard 1547(TM), IEEE Standard for Interconnecting Distributed Resources with Electric Power Systems, IEEE Standard 1547.2-2008.

[38] E. J. Currence, J. E. Plizga, and H. N. Nelson, "Harmonic resonance at a medium-sized industrial plant," in *IEEE Transactions on Industry Applications*, vol. 31, no. 4, pp. 682–690, Jul.-Aug. 1995.

[39] M. Saito, T. Takeshita, and N. Matsui, "Modeling and harmonic suppression for power distribution systems," in *IEEE Transactions on Industrial Electronics*, vol. 50, no. 6, pp.1148–1158, Dec. 2003.

Md Shirajum Munir received the B.Sc.Eng. degree from the Islamic University of Technology (IUT), Gazipur, Bangladesh, in 2007, Ph.D. degree from University of Alberta, Edmonton, AB, Canada, in 2018. He is currently working as a Senior Technical Consultant, IIoT at Phillips 66, USA.

His research interests include distributed generation, distribution system power quality improvement, industrial internet of things (IIOT).

Yun Wei Li received the B.Sc. in Engineering degree in electrical engineering from Tianjin University, Tianjin, China, in 2002, and the Ph.D. degree from Nanyang Technological University, Singapore, in 2006.

In 2005, Dr. Li was a Visiting Scholar with Aalborg University, Denmark. From 2006 to 2007, he was a Postdoctoral Research Fellow at Ryerson University, Canada. In 2007, he also worked at Rockwell Automation Canada before he joined University of Alberta, Canada in the same year. Since then, Dr. Li has been with University of Alberta, where he is a Professor now. His research interests include distributed generation, microgrid, renewable energy, high power converters and electric motor drives. Dr. Li serves as Editor-in-Chief for *IEEE Transactions on Power Electronics Letters*. Prior to that, he was Associate Editor for *IEEE Transactions on Power Electronics*, *IEEE Transactions on Industrial Electronics*, *IEEE Transactions on Smart Grid*, and *IEEE Journal of Emerging and Selected Topics in Power Electronics*.

Dr. Li received the Richard M.Bass Outstanding Young Power Electronics Engineer Award from IEEE Power Electronics Society in 2013 and the second prize paper award of *IEEE Transactions on Power Electronics* in 2014. He is listed as a Highly Cited Researcher by the Web of Science Group.

Hao Tian received the B.S. and M.Eng. degrees in electrical engineering from Shandong University, Jinan, China, in 2011 and 2014, respectively, and the Ph.D. degree in energy system from University of Alberta, Edmonton, Canada, in 2019. Since 2019, he has been working as a Postdoctoral Research Fellow with University of Alberta.

His research interests include multilevel topology and PWM, high-power converter control, and power quality of hybrid AC-DC microgrid.